Wavelet Applications in Signal and Image Processing III, Proc. SPIE #2569, p. 196-207 (1995)

Image enhancement with symmetric Daubechies wavelets

J.-M. Lina[1,2] and L. Gagnon[1*]
[1]Nuclear Physics Lab., Univ. de Montréal
C.P. 6128 Succ. Centre-Ville, Montréal(Québec), H3C 3J7, Canada
[2]Atlantic Nuclear Services Ltd., Fredericton, New Brunswick, E3B 5C8, Canada

Abstract

It is shown that analyses based on Symmetric Daubechies Wavelets (SDW) lead to a multiresolution form of the Laplacian operator. This property, which is related to the complex values of the SDWs, gives a way to new methods of image enhancement applications. After a brief recall of the construction and main properties of the SDW, we propose a representation of the sharpening operator at different scales and we discuss the "importance of the phase" of the complex wavelet coefficients.

1. INTRODUCTION

Many current investigations in mathematical imaging consist in finding the optimal representation to perform specific enhancements by extracting the relevant information contained in an empirical signal. This question of *representation*, present in many fields of applied mathematics and physics, is indeed the cornerstone of the pionnering work of D. Marr in vision[1]. The "raw primal sketch" of an image he proposed was based on the multiscale edge representation obtained through the action of some operators of different sizes. More specifically, Marr and Hildreth[2] argued that the convolution of the image with the filter associated with the Laplacian of the two dimensional Gaussian at different scales constitutes the most satisfactory representation. Such a representation identifies edges with the *zero-crossings* of the filtered image. Physiological experiments[1] gave credit to this model of vision generally known as the "Marr conjecture". In a more computational approach to edge detection proposed by Canny[3], edges are located at the *local extrema* of the convolutions of the image with the directional first order derivatives of some smoothing function (*e.g.* a Gaussian kernel). Unlike the zero-crossing technique, the Canny's edge detector characterizes the strength of the discontinuities in the image intensity. The synthesis of those two approaches is due to Mallat and Zhong[4,5] who demonstrated that *zero-crossings* and *local extrema* are unified in a single mathematical framework: the wavelet theory of frames. They further established an iterative algorithm to restore the original signal from these sparse representations. The aim of the present work is to show that similar ideas can be developped with *orthogonal multiresolution bases with compact support* provided we use the symmetric Daubechies wavelets[6,7].

Being complex-valued, the symmetric Daubechies multiresolution analyses did not receive much attention from the signal processing community since the resulting representation of a real field, such as an image, is a redundant expansion with complex-valued coefficients. Needless to say, this is also true with the Fourier transform; however, the reality condition is rather trivial and establishes a simple identity between the Fourier modes. The present work investigates the same kind of relationship between the complex wavelet coefficients: on the basis of comparison with the standard real Daubechies analyses, we show that the "natural redundancy" given by the complex Daubechies analyses of a real field provides a "dual representation" combining zero-crossings and local extrema. In fact, this result relies on the existence of "hidden" differential operators underlying some complex Symmetric Daubechies Wavelets (SDW). This result has interesting potential applications in numerical simulations[8] and signal processing[9,10].

Pursuing the parallel with Fourier representation, we can also wonder where the essential information

*Present address: R&D Department, LORAL Canada Inc., 6111 Ave. Royalmount, Montréal (Québec), H4P 1K6, Canada

of a signal is located in the complex wavelet coefficients. In the context of Fourier analysis, this point has been mainly discussed by Oppenheim and Li[11] who investigated on the "importance of the phase in signals". In the same way, we find that most informations are encoded in the phase of the wavelet coefficients and we describe a "phase-only wavelet synthesis" algorithm that restore most of the signal from the "shrunk representation" suggested by Donoho and Johnstone[12].

The paper is organized as follows. Section 2 briefly describes the basics of the multiresolution analyses and the SDW solutions. More details and results can be found in Ref.[7,9]. In Section 3, we describe the differential operator underlying some complex symmetric Daubechies multiresolution bases in one and two dimensions. Applications to edge enhancements are discussed in Section 4. Denoising and "phase reconstruction" are presented in Section 5. Conclusion will follow.

Notation: The derivatives and partial derivatives are denoted by a superscript as in Eq.(14) and by $\partial_x^m f$, respectively. Complex conjugaison of z is written $\overline{z}$.

2. SYMMETRIC DAUBECHIES WAVELETS

A multiresolution analysis of $L^2(\mathbb{R})$ is a sequence of closed subspaces $V_j \subset L^2(\mathbb{R})$ such that

$$V_j \subset V_{j+1}, \quad \bigcap_j V_j = \{0\}, \quad \overline{\bigcup_j V_j} = L^2(\mathbb{R}), \tag{1a}$$

$$f(x) \in V_0 \Leftrightarrow f(x \Leftrightarrow 1) \in V_0, \quad f(x) \in V_j \Leftrightarrow f(2x) \in V_{j+1} \tag{1b}$$

A scaling function $\varphi \in V_0$ with unit integral exists such that $\{\varphi_{0,k}(x) \equiv \varphi(x \Leftrightarrow k), k \in \mathbb{Z}\}$ is an orthonormal basis of V_0 and, consequently, the set of functions

$$\varphi_{j,k}(x) = 2^{\frac{j}{2}} \varphi(2^j x \Leftrightarrow k) \tag{2}$$

is an orthonormal basis of the space V_j. Since $\varphi \in V_0 \subset V_1$, a sequence of complex-valued coefficients a_k exists such that $\sum a_k = 1$ and

$$\varphi(x) = 2 \sum_k a_k \ \varphi(2x \Leftrightarrow k) \tag{3}$$

Multiresolution aims to decompose $L^2(\mathbb{R})$ as

$$L^2(\mathbb{R}) = V_{j_0} \oplus \sum_{j \geq j_0} W_j \tag{4}$$

where the spaces W_j are defined as the orthogonal complement of V_j in V_{j+1}: $V_{j+1} = V_j \oplus W_j$. For a given scale j, the space W_j is generated by the set of orthonormal wavelets $\psi_j(x) = 2^{\frac{j}{2}} \psi(2^j x)$ associated with the multiresolution analysis. Since $\psi \in W_0 \subset V_1$, a sequence of complex-valued coefficients b_k exists such that:

$$\psi(x) = 2 \sum_k b_k \ \varphi(2x \Leftrightarrow k) \tag{5}$$

The choice $b_k = (\Leftrightarrow 1)^k \overline{a}_{1-k}$ insures that the set $\{\psi_j(x \Leftrightarrow 2^{-j} k), k \in \mathbb{Z}\}$ is an orthonormal basis of W_j. In general, a field with finite energy will be "empirically known" at some scale and approximated in some $V_{j_{max}}$,

$$f(x) = \sum_k c_k^{j_{max}} \varphi_{j_{max},k}(x) \tag{6}$$

The discrete multiresolution analysis of f consists in the computation of the coefficients of the expansion

$$f(x) = \sum_k c_k^{j_0} \varphi_{j_0,k}(x) + \sum_{j=j_0}^{j_{max}-1} \sum_k d_k^j \psi_{j,k}(x) \tag{7}$$

where j_0 is a given low resolution scale. The coefficients in the previous expansion are computed through the orthogonal projection of the field over the multiresolution basis:

$$c_k^j = \langle \varphi_{j,k} | f \rangle, \qquad d_k^j = \langle \psi_{j,k} | f \rangle \tag{8}$$

Using the previous definition, we have the well-known *fast wavelet decomposition algorithm* (FWT) composed with the low-pass projection $V_j \to V_{j-1}$ and the high-pass projection $V_j \to W_{j-1}$:

$$c_n^{j-1} = \sqrt{2} \sum_k \bar{a}_{k-2n} c_k^j, \qquad \text{and} \qquad d_n^{j-1} = \sqrt{2} \sum_k \bar{b}_{k-2n} c_k^j \tag{9}$$

Conversely, any elements of V_{j-1} and of W_{j-1} can combine to give a unique vector in V_j; this reconstruction is expressed by the inverse FWT:

$$c_n^j = \sqrt{2} \sum_k a_{n-2k} c_k^{j-1} + \sqrt{2} \sum_k b_{n-2k} d_k^{j-1} \tag{10}$$

The Symmetric Daubechies Wavelets are subject to the following constraints:
(*i*) Compactness of the support of φ: We require that φ (and consequently ψ) has a compact support inside the interval $[\Leftrightarrow J, J+1]$ for some integer J that is, $a_k \neq 0$ for $k = \Leftrightarrow J, \Leftrightarrow J+1, \ldots, J, J+1$.
(*ii*) Orthogonality of the $\varphi(x \Leftrightarrow k)$: This condition defines in a large sense the Daubechies wavelets. Defining the polynomial

$$F(z) = \sum_{n=-J}^{J+1} a_n \, z^n, \quad \text{with } F(1) = 1 \tag{11}$$

where z is on the unit circle, $|z| = 1$, the orthonormality of the set $\{\varphi_{0,k}(x), k \in \mathbb{Z}\}$ can be stated through the following identity

$$P(z) \Leftrightarrow P(\Leftrightarrow z) = z \tag{12}$$

where the polynomial $P(z)$ is defined as

$$P(z) = z F(z) \overline{F(z)} \tag{13}$$

(*iii*) Accuracy of the approximation (6): To maximize the regularity of the functions generated by the scaling function φ, we require the vanishing of the first J moments of the wavelet or, in terms of the polynomial (11),

$$F'(\Leftrightarrow 1) = F''(\Leftrightarrow 1) = \ldots = F^{(J)} = 0 \tag{14}$$

The usual Daubechies wavelets[13] are the real polynomial solutions of Eqs.(12) and (14). They differ from each other through their degree of symmetry and, in general, the standard Daubechies wavelet (DAUBn) is the "least asymmetric" solution ($n = 2J+2$ being the length of the filters).
(*iv*) Symmetry: This condition amounts to have $a_k = a_{1-k}$ and can be written as

$$F(z) = z \, F(z^{-1}) \tag{15}$$

As anticipated by Lawton, only *complex-valued* solutions of φ and ψ, under the four above constraints, can exist, and for J even, only. The first solutions (from $J = 0$ to $J = 8$) were described in Ref.[7] by using the parametrized solutions of Eqs. (12), (14) and (15). The solutions have also been investigated in the spirit of the original Daubechies approach, *i.e.* by inspection of the roots of some so-called "valid polynomial"[6,10] that satisfies Eq.(12). Such a polynomial is defined by

$$P_J(z) = \left(\frac{1+z}{2}\right)^{2J+2} p_J(z^{-1}) \tag{16}$$

where

$$p_J(z) = \sum_{j=0}^{2J} r_j (z+1)^{2J-j} (z \Leftrightarrow 1)^j, \text{ with } \begin{cases} r_{2j} = (\Leftrightarrow 1)^j 2^{-2J} \binom{2J+1}{j}, \\ \\ r_{2j+1} = 0 \end{cases}, \quad j = 0, 1, \ldots, J \tag{17}$$

Straightforward algebra shows that $P_J(z)$ does satisfy Eq.(12).

The $2J$ roots of $p_J(z)$ displays obvious symmetries: the conjugate and the inverse of a root are also roots and no root are of unit modulus. If we denote by $x_{k=1,2,\ldots,J}$ the roots inside the unit circle ($|x_k| < 1$) and $\bar{x}_k = x_{J+1-k}$, then

$$p_J(z) = \prod_{k=1}^{J} \left(\frac{z \Leftrightarrow x_k}{1 \Leftrightarrow x_k}\right) \prod_{k=1}^{J} \left(\frac{z \Leftrightarrow \bar{x}_k^{-1}}{1 \Leftrightarrow \bar{x}_k^{-1}}\right) \tag{18}$$

and the low-pass filter $F(z)$ can be written as:

$$F(z) = \left(\frac{1+z}{2}\right)^{1+J} p(z^{-1}), \text{ with } p(z) = \prod_{m \in R} \left(\frac{z \Leftrightarrow x_m}{1 \Leftrightarrow x_m}\right) \prod_{n \in R'} \left(\frac{z \Leftrightarrow \bar{x}_n^{-1}}{1 \Leftrightarrow \bar{x}_n^{-1}}\right) \tag{19}$$

where R, R' are two arbitrary subsets of $\{1, 2, 3, \ldots, J\}$. The spectral factorization of $P(z) = zF(z)\overline{F}(z)$ implies $p_J(z) = z^J p(z^{-1})\overline{p(z)}$ which leads to the following constraint on R and R':

$$k \in R \Longleftrightarrow k \notin R' \tag{20}$$

This selection of roots fulfills the conditions *(i),(ii)* and *(iii)*. As an example, $R = \{1, 2, 3, \ldots, J\}$ and $R' = \emptyset$ corresponds to the DAUBn solution with $n = 2J + 2$. The addition of the symmetry condition *(iv)* defines a subset of solutions of Eq.(20). It corresponds to the constraint

$$k \in R \Longleftrightarrow J \Leftrightarrow k + 1 \in R' \text{ and } k \notin R' \tag{21}$$

For any even value of J, this defines a subset of $2^{\frac{J}{2}}$ complex solutions in the original set of "Daubechies wavelets" (2^J elements, complex or real). Notice that a complex conjugate of a solution is also a solution.

In the present work, we will consider a particular family of solutions, the so-called SDWJ Daubechies wavelets, that correspond to the following selection of roots:

$$R = \{1, 3, 5, \ldots, 2k+1, \ldots, J \Leftrightarrow 1\}, \quad R' = \{2, 4, \ldots, 2k, \ldots, J\} \tag{22}$$

that clearly satisfies the constraints (21). The complex scaling function and wavelet will be written as

$$\varphi(x) = h(x) + i\, g(x) \quad \text{and} \quad \psi(x) = w(x) + i\, v(x) \tag{23}$$

where h, g, w and v are all real functions. Figures 1,2 and 3 show examples of h, g, w and v for $J = 2, 4$ and 12. The filter coefficients $\sqrt{2}\, a_k$ for SDW2 and SDW4 are:

k	J=2	J=4
0	$0.662912 + 0.171163i$	$0.643003 + 0.182852i$
1	$0.110485 \Leftrightarrow 0.085581i$	$0.151379 \Leftrightarrow 0.094223i$
2	$\Leftrightarrow 0.066291 \Leftrightarrow 0.085581i$	$\Leftrightarrow 0.080639 \Leftrightarrow 0.117947i$
3	0.000000	$\Leftrightarrow 0.017128 + 0.008728i$
4	0.000000	$0.010492 + 0.020590i$

To conclude this section, we recall that the bi-dimensional multiresolution analysis is built from the tensor product of two multiresolution spaces V_i. We thus have one scaling function $\varphi(x)\varphi(y)$ complemented with three wavelets $\psi(x)\varphi(y), \varphi(x)\psi(y)$ and $\psi(x)\psi(y)$. We will write these complex-valued basis function as

$$\Phi(x,y) = \varphi(x)\varphi(y) = \Theta(x,y) + i\,\Psi(x,y), \tag{24}$$
$$\Psi^0(x,y) = \psi(x)\psi(y) = \xi_0(x,y) + i\,\zeta_0(x,y), \tag{25}$$
$$\Psi^1(x,y) = \psi(x)\varphi(y) = \xi_1(x,y) + i\,\zeta_1(x,y), \tag{26}$$
$$\Psi^2(x,y) = \varphi(x)\psi(y) = \xi_2(x,y) + i\,\zeta_2(x,y), \tag{27}$$

and expansions like (6) and (7) now generalize as

$$I(x,y) = \sum_{m,n} c_{m,n}^{j_{max}} \Phi_{j_{max},m,n}(x,y) \tag{28}$$

$$= \sum_{k_1,k_2} c_{k_1,k_2}^{l} \Phi_{l,k_1,k_2}(x,y) + \sum_{i=0}^{2} \sum_{j=l}^{j_{max}-1} \sum_{k_1,k_2} d_{j,k_1,k_2}^{i} \Psi_{j,k_1,k_2}^{i}(x,y) \tag{29}$$

where $\Phi_{j,k_1,k_2}(x,y) = 2^j \Phi(2^j x \Leftrightarrow k_1, 2^j y \Leftrightarrow k_2)$ and $\Psi_{j,k_1,k_2}(x,y) = 2^j \Psi(2^j x \Leftrightarrow k_1, 2^j y \Leftrightarrow k_2)$. In the sequel, we denote by W_N the wavelet transform

$$\{c_{m,n}^{j_{max}}\} \overset{W_N}{\Leftrightarrow} \{c_{m,n}^{j_{max}-N}, \mathbf{d}_{j_{max}-N,m,n}, \mathbf{d}_{j_{max}-2,m,n}, \ldots \mathbf{d}_{j_{max}-1,m,n}\} \tag{30}$$

where $\mathbf{d} = (d^0, d^1, d^2)$.

3. SOME PROPERTIES OF THE SYMMETRIC DAUBECHIES WAVELETS

In addition to the vanishing of the odd centered moments of the scaling function (due to the symmetry with respect to $x = 1/2$), *i.e.*

$$\int dx\, \bar{\varphi}(x)\, (x \Leftrightarrow \frac{1}{2})^{2i+1} = 0 \tag{31}$$

we can show that

$$\int dx\, h(x)\, (x \Leftrightarrow \frac{1}{2})^{2} = 0. \tag{32}$$

This result implies that the real part of φ has *always* its first three moments equal to 0. The complex scaling function is thus built from a "good" interpolating function $h(x)$ in the real part and from an admissible wavelet (the integral vanishes) $g(x)$ with one vanishing moment, in the imaginary part. In fact, this observation can be justified in a more analytical way. At least for the first values of J ($J < 12$), it has been shown in Ref.[10] that the complex scaling function is accurately approximated by

$$\varphi(x) \simeq (1 + i\alpha\partial_x^2)\, h(x) \tag{33}$$

where α is a small number that can be exactly computed from the coefficients a_k (α = -0.16 (J=2), -0.089 (J=4), -0.047 (J=12)). The approximation is very accurate on most of the frequency range $[0, \pi]$, where π is the normalized Nyquist frequency.

Similarly, the complex wavelet $\psi(x)$ is also well approximated by[10]

$$\psi(x) \simeq (1 + i\kappa + i\beta\partial_x^2)\, w(x), \text{ and } w(x) \simeq \mu\partial^{J+1} h(x) \tag{34}$$

where κ, β and μ can be exactly computed from the first non vanishing moments of ψ. Again, those identities are essentially verified on the frequency domain defined by the sampling rate.

Let us now turn to the bi-dimensional case. The real and imaginary parts of the scaling function are

$$\begin{cases} \Theta(x,y) = h(x)h(y) \Leftrightarrow g(x)g(y) \simeq G(x,y) \\ \Psi(x,y) = h(x)g(y) + g(x)h(y) \simeq \alpha \triangle G(x,y) \end{cases} \tag{35}$$

where $G(x,y)$ denotes the real smoothing kernel $h(x)h(y)$. We see that in one hand the real part of the 2-d scaling function is close (because $\alpha^2 << 1$) to the smoothing kernel $G(x,y)$ while, on the other hand, the imaginary part is proportional to the Laplacian of $G(x,y)$: $\Psi(x,y)$ is thus the "Marr wavelet" associated with $\Theta(x,y) \simeq G(x,y)$.

4. A SHARPENING ENHANCEMENT ALGORITHM

The simultaneous presence of a smoothing kernel and its Laplacian in the complex scaling function can be exploited to define some elementary operations on the wavelet coefficients. Since the real and imaginary parts of the wavelet transform coefficients of some *real* image correspond to the convolution of the original field with the real part and the imaginary part respectively of $\Phi_{j,m,n}(x,y)$, we then have access to the (multiscaled) smoothed Laplacian of the image.

Let us consider an image, *i.e* a real matrix $I_{m,n}$, and the bi-dimensional (complex valued) field $f(x,y)$ defined by the expansion (28) with $c_{m,n}^{j_{max}} = I_{m,n} \in \mathbb{R}$. The field $f(x,y)$ is a particular point in the space $R_{j_{max}}$ defined as the set of all fields constructed with real scaling coefficients at scale j_{max}. We denote by P_R the orthogonal projector on this space; it is simply defined by keeping the real part of the scaling coefficients only:

$$P_R\Big(\sum_{m,n}(\tilde{h}_{m,n}^{j_{max}} + i\tilde{g}_{m,n}^{j_{max}})\Phi_{j_{max},m,n}(x,y)\Big) = \sum_{m,n}\tilde{h}_{m,n}^{j_{max}}\Phi_{j_{max},m,n}(x,y) \tag{36}$$

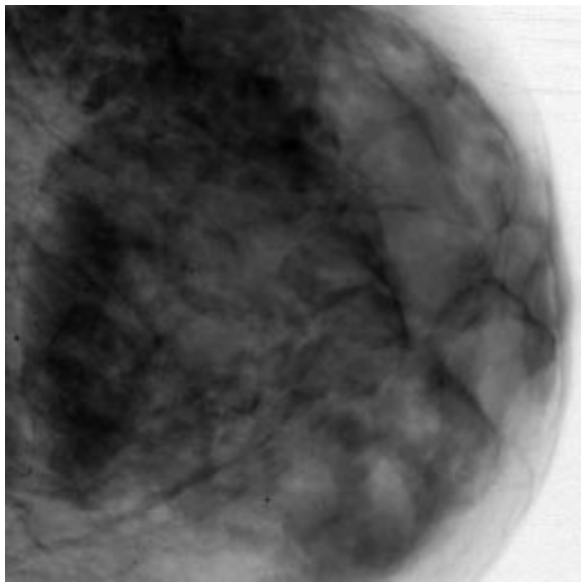

Figure 4: Original mammogram

Let us now define a smoothing operator $Z: R_{j_{max}} \to R_{j_{max}+1}$ by the inverse wavelet transform with the real part of the SDW filters only. The image Zf is at resolution twice of the original image, without spurious high-frequency components. Then, the complex wavelet decomposition $W_1 Zf$ gives, in the imaginary part of the scaling coefficients, a good estimate of the Laplacian of $I_{m,n}$.

To illustrate this algorithm, we consider the sharpening operator, $f \to \tilde{f} = f \Leftrightarrow \rho\triangle f$. It can be implemented at the finest resolution scale through

$$c_{m,n}^{j_{max}} \to \tilde{c}_{m,n}^{j_{max}} = c_{m,n}^{j_{max}} + \frac{\rho}{\alpha} g_{m,n}^{j_{max}} \tag{37}$$

followed by the projection of this enhanced complex field on $R_{j_{max}}$:

$$\tilde{I}(x,y) = P_R\Big(\sum_{m,n}\tilde{c}_{m,n}^{j_{max}}\Phi_{j_{max},m,n}(x,y)\Big) = \sum_{m,n}\tilde{h}_{m,n}^{j_{max}}\Phi_{j_{max},m,n}(x,y) \tag{38}$$

This algorithm can easily be generalized for a non-linear multiscale enhancement by considering a N level

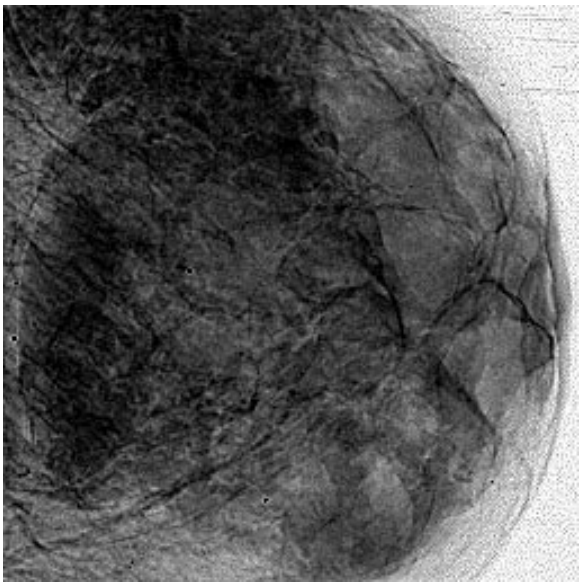

Figure 5: Processed mammogram with $N = 3$, $J = 2$ and $\rho = \{20, 5, 1\}$

decomposition of Zf and by applying the adapted enhancement

$$c^j_{m,n} \rightarrow c^j_{m,n} + \frac{\rho_j}{2^{2(j_{max}-j)}\alpha} g^j_{m,n} \tag{39}$$

at each level of the reconstruction. The coefficients $c^j_{m,n}$ are induced by the synthesis process, whereas the coefficients $g^j_{m,n}$ are calculated during the decomposition process. The sharpening parameter ρ is now scale dependent ($\rho \rightarrow \rho_j$). Preliminary tests of this algorithm have been performed on low-resolution and low-contrast mammographic images. A typical result is shown on Figure 5. The original picture (Figure 4) has a resolution of 400 micron/pixel and is coded at 2 byte/pixel. We have processed it with SDW of order $J = 2$, over a 3-level multiresolution decomposition ($N = 3$) and with enhancement parameters $\rho = \{20, 5, 1\}$. The local contrast between the low and high X-ray attenuation regions has been improved significantly in the processed mammogram (Figure 5). For better visual comparison of the sharpening enhancement, we have clipped the pixels value of the processed mammogram with low and high values of the original window range. Let us mention that other efficient multiscale sharpening transformations have been proposed in the recent past[14]. The main difference here in the present work is the orthogonality property of the SDW transform. We recall that the SDW bases are not derived from a representation that allows specific enhancements. On the contrary, we have shown that the Laplacian was inherent to this particular orthogonal basis.

5. SHRINKAGE AND PHASE

Other important non-linear transformations in image processing are regression modeling and denoising. Mostly advocated by Donoho and Johnstone[12], the wavelet regression estimators, based on orthogonal multiresolution bases and the shrinkage of the empirical wavelet coefficients, provide near-optimal estimates of the true signal. Apart from the choice of the basis, the wavelet regression technique suggested by the authors of the Ref.[12] relies on the definition of the thresholding rule (hard or soft) and the selection of the appropriate threshold (optimal or universal). In the present work, we adopt soft-thresholding with universal threshold, *i.e VisuShrink*. Based on the amplitude of the wavelet coefficients, this regression estimator can be directly implemented on the complex coefficients. Starting from the empirical expansion

$$f_0(x, y) = \sum_{m,n} I_{m,n} \Phi_{j_{max},m,n}(x, y) \tag{40}$$

we consider the field

$$\tilde{f}_0(x,y) = \sum_{m,n} \tilde{I}_{m,n} \Phi_{j_{max},m,n}(x,y) \tag{41}$$

with

$$\tilde{I} = (W_N^{-1}\, \mathcal{T}\, W_N)\, I \tag{42}$$

where the shrinkage operator $\mathcal{T}$,

$$\mathcal{T}(\{c_{m,n}^{j_{max}-N}, \mathbf{d}_{j_{max}-N,m,n}, \ldots \mathbf{d}_{j_{max}-1,m,n}\}) = \left(c_{m,n}^{j_{max}-N}, \eta(\mathbf{d}_{j_{max}-N,m,n}), \ldots, \eta(\mathbf{d}_{j_{max}-1,m,n})\right) \tag{43}$$

is defined with

$$\eta(\mathbf{d}) = (\eta_0(d^0), \eta_1(d^1), \eta_2(d^2)), \quad \eta_i(d^i) = sgn(d^i)(|d^i| \Leftrightarrow t_i)\, I(|d^i| > t_i) \tag{44}$$

$I(x)$ is the indicator function. The universal thresholds t_i are the most important parameters of this regression method. There are such that the universal estimate is noise-free, *i.e* $t_i = \sqrt{2log(n^2)}\sigma_i$, n^2 being the size of the image and σ_i the noise variance directly estimated from the wavelet coefficients $d^i_{j_{max}-1,m,n}$. A simple estimation is given[11] by $\sigma_i = median(|d^i_{j_{max}-1,m,n}|)/0.6745$.

Figure 6: Noisy moon, psnr = 16.8db

In most application where the noise is important, the usual wavelet regression techniques tend to underfit the true signal by shrinking too many coefficients[15]. The same observation is made with the SDW when we consider the real image produced by the scaling coefficients of $P_R\tilde{f}_0$ (see Figure 6 and Figure 7). However, in many experiments we noticed that local artefacts in the universal estimate were in correspondance with transients in the imaginary part of the scaling coefficients of $\tilde{f}_0$. This observation leads us to consider the improvement of the universal estimate by using the phase information contained in the wavelet coefficients and left untouched by the shrinkage operation.

Given an image and the empirical complex wavelet coefficients $\{c_{m,n}^{j_{max}-N}, \mathbf{d}_{j_{max}-N,m,n}, \ldots \mathbf{d}_{j_{max}-1,m,n}\}$ associated with f_0, we define the space , $_{j_{max}}$ of all the fields $f(x,y)$ such that

$$f(x,y) = \sum_{k_1,k_2} c_{k_1,k_2}^{j_{max}-N}\, \Phi_{l,k_1,k_2}(x,y) + \sum_{i=0}^{2} \sum_{j=1}^{N} \sum_{k_1,k_2} f^i_{j_{max}-j,k_1,k_2} \Psi^i_{j_{max}-j,k_1,k_2}(x,y) \tag{45}$$

Figure 7: "Visu-Shrinkage" of moon with SDW4, psnr = 26.4db

with

$$Arg(f^i_{j,m,n}) = Arg(d^i_{j,m,n}), \quad \forall i,j,m,n \tag{46}$$

We denote by P_Γ the orthogonal projector on $,_{j_{max}}$: it is simply given by the orthogonal projections of the complex wavelet components $f^i_{j,m,n}$ on the line defined by the phase $Arg(d^i_{j,m,n})$. Of course, the initial empirical field f_0 and the estimate $\tilde{f}_0$ (whatever the thresholding rule and the threshold used) belong to $,_{j_{max}}$. This space and the space $R_{j_{max}}$ are both convex spaces and the intersection $,_{j_{max}} \cap R_{j_{max}}$ contains, at least, the field f_0 (see Figure 7).

Let us consider the sequence of real images $I^l_{m,n}$ defined by

$$\sum_{m,n} I^l_{m,n}\, \Phi_{j_{max},m,n}(x,y) = \left(P_R P_\Gamma\right)^l \tilde{f}_0 \tag{47}$$

Well-known theorems[16] prove the convergence of this sequence as $l \to \infty$. The alternate projections converge to a point in $,_{j_{max}} \cap R_{j_{max}}$. The complete characterisation of this limit is still an open problem but few comments are in order. First, as illutrated by Figure 9, the reconstructed image is close to the original one. The "phase reconstruction algorithm" restores the edges and the small features blured by the shrinkage. During the iterative projections, the PSNR starts increasing and finally decreases slowly after few iterations. Various simulations have shown that the (coherent) true signal was mainly reconstructed during the first hundreds iterations. Second, the choice of the SDW wavelet and the definition of the initial estimate $\tilde{f}_0$ apparently have no effect on the limit; however, they affect the speed of convergence. Finally, 1-d simulations have shown that only some specific wavelet coefficients shrunk to zero were restored during the process. Those partial results indicate that, provided an appropriate shrinkage (related to the a priori knowledge on the noise), the "phase reconstruction algorithm" improves the initial estimate by adapting the thresholding rule to the coherence of the signal.

6. CONCLUSION

We have described a simple multiresolution sharpening enhancement algorithm based on the "hidden" Laplacian kernel of the Symmetric Daubechies Wavelet analyses. Beside this operation that acts only on the scaling coefficients, we have discussed the importance of the phase in the wavelet coefficients. Most

information is indeed encoded in this phase of the coefficients and it is worth mentioning that experiments also demonstrate the crucial role of the phase in the human system vision[17]. Quite remarkably, the condition of symmetry, which is required in image analysis for very practical reasons, leads to multiresolution representations that seem to be of main relevance in Nature.
The apparent price for the symmetry of the Daubechies Wavelets, that is the complex-valued Daubechies scaling functions, might turn to suggest unexpected applications of the Daubechies wavelets in image analysis.

7. ACKNOWLEDGMENTS

J.M.L. wishes to thank Stéphane Mallat for discussions about the "phase reconstruction" algorithm. This work was supported in part by the Natural Sciences and Engineering Research Council (NSERC) of Canada.

8. REFERENCES

1. D. Marr, *Vision*, W.H. Freeman, San Francisco, 1982.
2. D. Marr and E. Hildreth, "Theory of edge detection", Proc. Royal So. London, vol.207, p.187-217, 1980.
3. J. Canny, "A computational approach to edge detection", IEEE Trans. Pattern Anal. Machine Intell., vol.8, p.679-698, 1986; I.D.G. Macleod, "On finding structures in picture" in Picture Language Machines, S. Kaneff ed., Academic Press, New York, p.231, 1970.
4. S. Mallat, "Zero-crossings of a wavelet transform", IEEE Trans. Info. Theory, vol.37, p.1019-1033, 1991.
5. S. Mallat and S. Zhong, "Characterization of signals from multiscale edges", IEEE Trans. Patt. Anal. Machine Intell., vol.14, p.710-732, 1992.
6. W. Lawton, "Applications of Complex Valued Wavelet Transforms to Subband Decomposition", IEEE Trans. on Signal Proc., vol.41, p.3566-3568, 1993.
7. J.M. Lina and M. Mayrand, "Complex Daubechies Wavelets", to be published in App. Comp. Harmonic Anal., vol.2, 1995.
8. L. Gagnon and J.M. Lina, "Symmetric Daubechies wavelet and numerical solution of NLS equations", Jour. Phys. A, vol.27, p.8207-8230, 1994.
9. B. Belzer, J.M. Lina and J. Villasenor, "Complex linear phase filters for efficient image coding", to be published in IEEE Trans. on Signal Proc., 1995; L. Gagnon, J.M. Lina and B. Goulard, "Sharpening Enhancement of Digitalized Mammograms with Complex Symmetric Daubechies Wavelets", submitted to the 17^{th} Ann. Inter. Conf. of the IEEE Eng. in Medecine and Biology Society, Montreal, Sept. 1995.
10. J.-M. Lina, "From Daubechies to Marr", ANS-PhysNum Report 20, Univ. of Montreal, March 1995.
11. A.V. Oppenheim and J.S. Li, "The importance of phase in signals", Proc. IEEE, vol.69, p.529-541, 1981.
12. D. Donoho and I. Johnstone, "Adapting to unknown smoothness via wavelet shrinkage", to be published in J. Amer. Statist. Assoc., 1995.
13. I. Daubechies, "Orthonormal bases of compactly supported wavelets", Comm. Pure Appl. Math., vol.41, p.909-996, 1988; *Ten lectures on Wavelets*, SIAM, CBMS Series, 1992.
14. A. F. Laine, S. Schuler, J. Fan and W. Huda, "Mammographic Feature Enhancement by Multiscale Analysis", IEEE Transactions on Medical Imaging vol. 13, pp. 725-740, 1994;J. Lu, D. M. Healy Jr. and J. B. Weaver, "Contrast Enhancement of Medical Images Using Multiscale Edge Representation", SPIE vol. 2242 Wavelet Applications, pp. 711-719, 1994
15. G. P. Nason, "Wavelet regression by cross-validation", Tech. Report 447. Dept. of Statistic, Stanford (April 1994), and references therein.
16. D.C. Youla and H. Webb, "Image restoration by the method of convex projections", IEEE Trans. on Medical Imaging, vol. 1 (2), p.81-94, 1982.
17. A. Burgess and H. Ghandeharian, "Visual signal detection. I. Ability to use phase information", J. Opt. Soc. Am., vol.1, p.900-905, 1984.

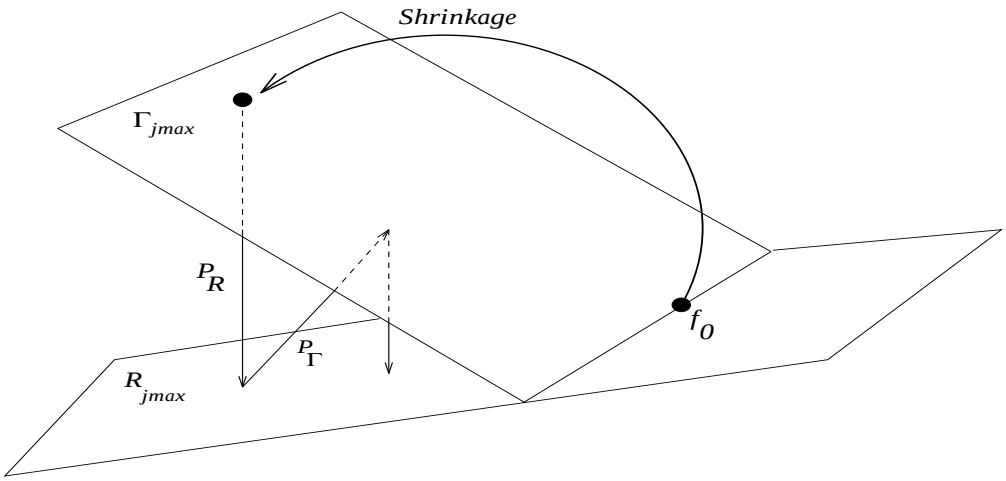

Figure 8: Phase reconstruction by alternating projections on affine spaces , $_{j_{max}}$ and $R_{j_{max}}$

Figure 9: Shrinkage and phase restoration of moon with 300 iterations, psnr = 26.5db